

Multielectron Effects on Single-Electron Strong Field Ionization

Chunlei Guo*

*Condensed Matter and Thermal Physics Group, Materials Science and Technology Division,
Los Alamos National Laboratory, Los Alamos, New Mexico 87545*

(Received 12 January 2000)

An apparently simple phenomenon of single-electron strong field ionization involves subtle factors related to multielectron effects. A single electron in an atom or molecule can feel a distinctly different screening strength when exposed to strong fields as opposed to weak fields, and this electron screening due to multielectron motion influences single-electron ionization. The concept and a corresponding model developed in the paper allow a generalization of the Ammosov-Delone-Krainov model for predicting strong field ionization rates of more complicated atoms and molecules. This general approach explains the recently observed anomalous low single ionization rate in O_2 .

PACS numbers: 32.80.Rm, 33.80.Rv, 42.50.Hz

The understanding of photoionization processes is the foremost problem in strong field atomic and molecular physics, since ionization always occurs when electrons in atoms or molecules are exposed to an ultrashort strong laser field that is comparable in strength to their Coulomb binding potentials. All the major problems studied in the current field, such as single- and multiple-electron ionization, above-threshold ionization, high harmonic generation, molecular dissociation and ionization, and photoelectron spectroscopy, are derived directly or indirectly from electron ionization. Needless to say, therefore, a solid understanding of the detailed ionization process forms the foundation of strong field laser physics.

Most of the single-electron strong field ionization of rare gas atoms and related phenomena can be relatively well understood by the single active electron (SAE) approximation. Time-dependent quantum mechanical calculations using the SAE approximation have been shown to provide accurate single ionization rates, above-threshold ionization spectra, and angular distributions for rare gas atoms in strong laser fields [1–4]. In the tunneling regime [5], the SAE-based Ammosov-Delone-Krainov (ADK) tunneling model also provides an accurate fit to single- and sequential multiple-electron ionization rates of rare gas atoms [6]. The model is relatively simple: different atoms are characterized only by their ionization potential (I_p) and the effective quantum numbers obtained from weak field measurements; apparently, the details of the electronic structure are unimportant. However, most of the subjects studied extensively with this model are the rare gas atoms that all have similar closed shell electronic structures.

Despite the success in explaining the phenomena of the single-electron response of rare gas atoms in strong fields, the understanding of single-electron strong field ionization in molecules encounters great difficulties and remains unclear. Previous studies provide evidence that many aspects of strong field ionization of molecules are similar to those of atoms. In the multiphoton regime [5], photoelectron spectroscopy of N_2 showed atomiclike multiphoton resonance similar to Ar, as well as details of the electronic

structure of N_2^+ [7]. In the tunneling regime, ion yields of several simple molecules in $10.6 \mu\text{m}$ CO_2 laser radiation have been found to agree with the ADK model [8]. This implies that, in the absence of vibrational resonance with the CO_2 laser, “simple” molecules are ionized through tunneling as if they were structureless atoms with an I_p equivalent to that of the molecular ground state [8]. More recently, however, with 800 nm Ti:sapphire laser radiation, O_2^+ was found to have a significantly lower ion yield signal compared to Xe^+ [9], which has the same single I_p as O_2 . This anomalous behavior of O_2 is further corroborated in our measurements, but the low ion signal is not observed in the diatomic molecule N_2 [10]. This indicates that the peculiar behavior of O_2 is not a consequence of some molecular nature. Rather, the fact that N_2 behaves like a structureless atom for both single and double ionization, while O_2 shows distinct nonatomiclike behavior having both low single and nonsequential double ionization rates, indicates that the detailed electronic structure plays key roles in influencing the strong field excitation and ionization, as manifested in recent experiments covering a variety of strong field phenomena, since N_2 has a closed shell electronic structure with the outermost two-electron wave function spatially symmetric distributed, while O_2 has a half-filled open shell electronic structure with the outermost two-electron wave function spatially antisymmetric distributed [10–12].

More recently, we performed *ab initio* 1D two-electron quantum mechanical calculations on two simplified model atoms with either a spatially symmetric wave function or a spatially antisymmetric wave function to approximately characterize the valence electron distribution in N_2 and O_2 [13]. Not only are the influences of the spatial symmetry of wave function and electronic structure on nonsequential double ionization reinforced in these calculations, but the single-electron ionization is also demonstrated to be a dynamic process correlating with the double ionization. This indicates that single-electron ionization is not an isolated process as described by the SAE approximation, rather, the motion of other electrons could play a role in influencing

this single-electron ionization. Unfortunately, the simplified model atoms do not fully represent the exact electronic structures of the molecules, and the underlying physics of how exactly single-electron motion is tied to multielectron effects cannot be understood directly from the *ab initio* calculations. The mechanism of single ionization needs further investigation.

It is of premier importance to confront and clarify single-electron ionization in molecules since it is the foundation of studying molecular behaviors in strong fields. In this paper, through the study of tunneling ionization of O_2 , multielectron effects are demonstrated, for the first time, playing a key role in determining the underlying physics of single-electron strong field ionization.

The ADK complex tunneling model is commonly used in predicating the ionization rate in the strong field tunneling regime [5]. In this model, the ionization rate in an ac field is given by, in atomic units [6],

$$W_{ac} = C_{n^*l^*}^2 f(l, m) \left(\frac{3F}{\pi E_0} \right)^{1/2} \left(\frac{2E_0}{F} \right)^{2n^* - |m| - 1} \times \exp\left(-\frac{2E_0}{3F}\right), \quad (1)$$

where F is laser field strength, and $E_0 = (2I_P)^{3/2}$ with I_P denoting the ionization potential. The atomic structure is introduced by the coefficients $f(l, m)$ and $C_{n^*l^*}$, where $f(l, m) = (2l + 1)(l + |m|)! [2^{|m|} (|m|)! (l - |m|)!]^{-1}$ and $C_{n^*l^*} = 2^{2n^*} [n^*(n^* + l^*)! (n^* - l^* - 1)!]^{-1}$. The value of $C_{n^*l^*}$ is expressed with effective quantum numbers, n^* and l^* , since the expression is known only for the hydrogen atom [14,15], where $n^* = z(2I_P)^{-1/2}$, with z denoting the final charge state, $l^* = n_0^* - 1$, with n_0^* the effective principal quantum number of the ground state for a given orbital quantum number l [16,17].

Ion yields of singly ionized O_2 and Xe in 30 fs, 800 nm linearly polarized light are reproduced from Ref. [10], as shown in Fig. 1. The experimental data can be modeled by integrating the ionization rate obtained from the ADK model over the measured pulse duration and focal volume. As explained in Ref. [10], absolute calibration of the laser intensity and the overall detection efficiency were first determined by fitting the Ar^+ linear polarization ion yield, which subsequently fix all the experimental parameters used in the ADK model fit. The model fit for different ionization species is characterized by changing only the final charge z and ionization potential I_P (effective quantum numbers also vary accordingly). In Fig. 1, rare gas ion Xe^+ is fitted by setting $z = 1$ and $I_P = 12.13$ eV (single I_P for Xe), and we can see that the ADK model fits Xe^+ very well in the high intensity range. In contrast, the O_2^+ signal is significantly lower than Xe^+ even though O_2 and Xe have nearly the same single I_P (O_2 , 12.06 eV; Xe, 12.13 eV). Note that the discussion in this paper concentrates on strong field tunneling ionization. In the case of singly ionized Xe and O_2 , tunneling ionization dominates at intensities above 1×10^{14} W/cm² according to

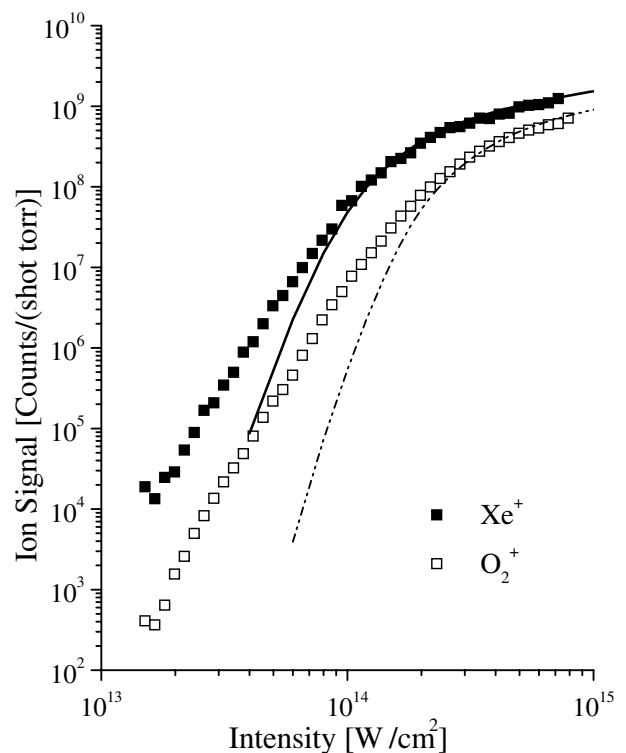


FIG. 1. Ionization yields for Xe^+ and O_2^+ for linearly polarized light. The full curve is the ADK model calculations using weak field single ionization potential of Xe. The dash-dotted curve fitting O_2^+ data uses an effective charge z^* of 1.4 and an I_P^* of 16.9 eV.

the Keldysh theory (Keldysh parameter < 1) [5]. As a tunneling model, the ADK model fitting will be based on the data in the high intensity range, especially in the saturation region where there is the least fitting bias based on the volume saturation effect [18]. Any deviation between the data and model fit in the lower intensity range comes from the multiphoton ionization component [5], which is not relevant to the discussion in this paper. As discussed in detail in Ref. [10], no effect has been found to explain the suppression of the O_2^+ signal in considering general differences between atoms and molecules, such as the possibilities of dissociative recombination through rescattering, general dissociation mechanism, the different polarizabilities between atoms and molecules, the presence of any accidental electronic resonance, and enhanced ionization due to electron localization in molecules at a critical internuclear separation. It is thus clear that the ion yield of O_2^+ is below that predicted by tunneling ionization [10].

In order to understand this discrepancy between the O_2^+ signal and the ADK model fitting, we consider the adjustable parameters in the ADK model: the final charge z and I_P . First we consider I_P : the I_P we use in the ADK model is the value obtained from previous weak field measurements. These methods typically include deducing Rydberg series limits, weak electrical or optical field spectroscopy, and electron impact ionization experiments [19]. The time scale for ionizing an electron by a weak field

is much longer compared to strong field tunneling ionization. While a given electron is being ionized and moving away from the ion core in a weak field, there is a relatively long time for all the other electrons in weak fields to adjust their positions to minimize the energy. This change of electrons' position will induce a continuous variation of the strength of core screening and result in a changing mean field seen by this ionizing electron while it moves away from the core. Therefore, the weak field I_P is in fact a value averaged over this subtle and highly dynamic process. All the complexity of many-body problems and the dynamics of multielectron effects have been incorporated into this mean field value of I_P .

The tunneling ionization in strong laser fields, however, is a fundamentally different process compared to that of the weak fields, and challenges the traditional way we understand light-matter interactions. Many approximations based on perturbative or adiabatic process break down when an atom or molecule is exposed to an ultrashort intense laser pulse. In a strong laser field, electron tunneling ionization occurs within a half cycle of laser light. For 800 nm radiation, a half cycle is about 1.3 fs. The ionization, in fact, predominantly occurs only when the laser intensity reaches its peak value, which is only a fraction of the 1.3 fs. This time scale is already comparable to one period of a valence electron orbital in a large atom or molecule (the period of the $1s$ electron in the smallest atom, the hydrogen atom, is $\sim 2.42 \times 10^{-17}$ s, and the orbital period is proportional to $r^{3/2}$ with r denoting orbiting radius). During the ultrashort time interval in tunneling ionization, the change of other electrons' position due to the receding ionized electron will be small, and the subsequent core screening seen by this leaving electron will be much less effective compared to the weak field ionization.

The major difference, resulting from the distinctly different ionization process between strong field and weak field experiments, is the strength of electron screening of the ion core. The application of the concept of electron screening is very powerful to simplify complicated many-body problems. The value of I_P itself (as indicated two paragraphs before) involves the electron screening, which is also the essence of many concepts in other collateral many-body phenomena, such as Debye shielding in plasma physics, the Thomas-Fermi model, the Lindhard theory, and the Fermi liquid theory used in condensed matter physics. The difficulty in fitting O_2^+ using the ADK model in fact comes from the absence of the values of an effective charge z^* and a corresponding ionization potential I_P^* in strong field ionization for some atoms or molecules (like O_2), which should not be the same as the weak field values due to the fundamentally different electron screening process. O_2 , for example, has a half-filled open shell structure. We know that the two outermost $1\pi_g$ valence electrons have the same spin direction because the ground state of O_2 is a triplet state. The symmetry of the spin part of the wave function restricts the spatial part of the wave function to be antisymmetric. Therefore, these

two outer electrons are located on the opposite sides of the core, as illustrated in Fig. 2. Pictorially speaking, as one of the outer electrons is tunneling ionized away from the core in a strong field, there will be little time for the other electron from the other side of the core to "jump over" and screen the core charge as effectively as in a weak field. Therefore, the ionizing electron in a strong field will see a higher net charge than that in a weak field, and ionization becomes harder and requires higher intensity. This is why a distinctly reduced yield of O_2^+ is observed in strong fields, as shown in Fig. 1. However, all the rare gas atoms and the diatomic molecule N_2 can still be well described by the ADK model using the I_P from the weak field measurements; this is because, unlike O_2 , the outermost electrons in rare gas atoms and N_2 are indistinguishably distributed uniformly around the core, and this leads to little difference between electron screening in strong fields and weak fields despite the different ionization process. Furthermore, it is also clear why the ion yield of O_2^+ can be fitted better with the ADK model using weak field I_P in 10.6 μm CO_2 laser radiation [8]. The period of the CO_2 laser field is more than 13 times longer than 800 nm Ti:sapphire radiation. Even though an electron still undergoes barrier tunneling in CO_2 radiation, the interaction time of laser field and molecule will be much longer than that in 800 nm radiation. Therefore, there is more time for the other outer electron in the $1\pi_g$ orbital of O_2 to adjust its position and shield the core charge more effectively. Thus, the differences between the effective charge (z^* vs z) and ionization potential (I_P^* vs I_P) of strong fields and weak fields in O_2 are much smaller in 10.6 μm radiation.

To find the effective z^* and I_P^* in strong fields, a classical estimation is described here for O_2 . As shown in Fig. 2, an O_2 molecule is simplified by the two outermost electrons 1 and 2, and the rest of the electrons and two nuclei are represented by a core with charge $z = +2$ in the center. In a strong field ionization limit, we use the diabatic approximation and assume the core and electron 1 remain fixed during the instantaneous tunneling ionization, and therefore, the work required for a laser field to overcome the Coulomb binding energy and boost electron 2 into continuum will be equal to the potential energy of electron 2 in this configuration. In atomic units, the potential of electron 2 is

$$V = -\frac{2}{r_0} + \frac{1}{2r_0}, \quad (2)$$

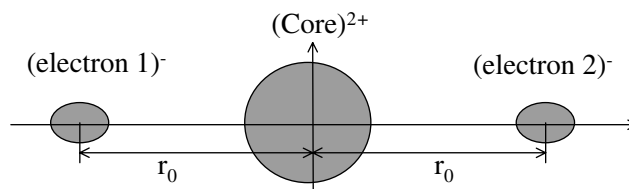


FIG. 2. Illustration of a simplified electronic configuration of O_2 .

where r_0 is the distance between electron 1 or 2 and the core center. Now we assume that the core and electron 1 combine into a new core with an effective charge z^* , and the potential energy of electron 2 in this mean field will be

$$V_{\text{eff}} = -\frac{z^*}{r_0}. \quad (3)$$

We set $V = V_{\text{eff}}$ to solve for z^* , and the result is 1.5. In this classical approximation, we can see that the ionized electron in O_2 does see a higher net charge in tunneling instantaneous ionization and therefore requires higher intensity to ionize. For weak field ionization in O_2 , however, even though the initial net charge seen by an outermost electron is still 1.5, as this electron moves relatively slowly away from the core, the other outer electron will have enough time to move towards the core to minimize the energy and reduce the net charge leading to a lower I_P . Since the outer electrons are uniformly distributed around the core in N_2 and rare gas atoms, the effective charge will still be one for strong field ionization using the same argument described above and, therefore, the ADK model is still valid for these species when fit with the values of final charge z and weak field I_P .

Now we fit the O_2^+ data (in Fig. 1) with the ADK model using an effective z^* and strong field I_P^* . Since ionization potential is proportional to the effective charge z^* , we vary I_P^* as $z^* \times 12.06$ eV (12.06 eV is the weak field I_P with net charge $z = 1$). By setting $z^* = 1.4$ and $I_P^* = 1.4 \times 12.06$ eV (note that effective quantum numbers, such as n^* and l^* , will also change accordingly), the ADK curve can fit the data very well (see Fig. 1) in the tunneling regime. The z^* of 1.4 is very close to the value of 1.5 obtained above with the classical frozen core calculations, and the small deviation can be understood as the contribution from the weaker electron screening in strong fields. By changing both z^* and I_P^* in this fashion, the ADK model fits the data over a larger intensity range compared to changing only z^* or I_P^* . The tunneling ionized electron in O_2 can be summarized as seeing a net charge z^* of 1.4 and a mean field I_P^* of 16.9 eV as it tunneling ionizes in a strong laser field. Therefore, the ADK model will still be valid in predicating ionization rates of more complicated atoms and molecules, as long as we take into account the detailed ionization processes occurring in strong fields.

In summary, it is clear now that the anomalous suppression of O_2^+ compared to Xe^+ is not anomalous at all; rather, it is just a natural consequence of strong field instantaneous tunneling ionization. We can see that the assumption of effective charge to be the final charge state and the value of the ionization potential obtained in previous weak field measurements are not always valid in strong field ionization. The criteria to determine this validity will be the detailed electronic structure and the electron screen-

ing process due to this detailed electronic structure. By carefully considering the individual ionization process, the ADK model (as a mean field model) can still be used in a complicated molecular system with a corrected effective charge and strong field ionization potential.

Although multielectron effects are discussed in this Letter through a specific case of studying the tunneling ionization of O_2 , it needs to be emphasized that the implications of this work are beyond an interpretation of the anomalous ionization behavior of O_2 , and the ultimate purpose of this paper is twofold. First, it is shown to be of importance to carefully consider the multielectron effects in studying any ionization phenomena in both strong and weak fields. Second, the importance of many-body (MB) effects is addressed here in atomic and molecular systems. The study of MB problems is crucial to understand a system involving a large number of interacting particles, e.g., solids. The effects of MB and electron correlation recently also attracted significant attention in strong field atomic and molecular physics through the study of nonsequential ionization where at least two electrons dominate the process [4,12,20,21]. The problem discussed in this paper, however, brings the study of MB problems into a case in which even a smaller number of particles (only one) dominates and provides another testing ground to understand the MB effects at the most fundamental level.

I would like to acknowledge discussions with G. N. Gibson.

*Electronic address: cguo@lanl.gov

- [1] K. C. Kulander, Phys. Rev. A **35**, 445 (1987).
- [2] K. J. Schafer *et al.*, Phys. Rev. Lett. **70**, 1599 (1993).
- [3] B. Yang *et al.*, Phys. Rev. Lett. **71**, 3770 (1993).
- [4] B. Walker *et al.*, Phys. Rev. Lett. **73**, 1227 (1994).
- [5] L. V. Keldysh, Sov. Phys. JETP **20**, 1307 (1965).
- [6] M. V. Ammosov *et al.*, Sov. Phys. JETP **64**, 1191 (1986).
- [7] G. N. Gibson *et al.*, Phys. Rev. Lett. **67**, 1230 (1991).
- [8] S. L. Chin *et al.*, J. Phys. B **25**, L249, (1992); T. D. G. Walsh *et al.*, J. Phys. B **27**, 3767 (1994).
- [9] A. Talebpour *et al.*, J. Phys. B **29**, L677 (1996).
- [10] C. Guo *et al.*, Phys. Rev. A **58**, R4271 (1998).
- [11] C. Guo *et al.*, Phys. Rev. Lett. **82**, 2492 (1999).
- [12] C. Guo *et al.*, Phys. Rev. A **61**, 33413 (2000).
- [13] C. Guo *et al.*, Phys. Rev. A **62**, 15402 (2000).
- [14] L. D. Landau and E. M. Lifshitz, *Quantum Mechanics* (Pergamon, Oxford, 1977), 3rd ed.
- [15] A. M. Perelomov and V. S. Popov, Sov. Phys. JETP **25**, 336 (1967).
- [16] G. Simons, J. Chem. Phys. **55**, 756 (1971).
- [17] M. G. Littman *et al.*, Phys. Rev. Lett. **41**, 103 (1978).
- [18] M. D. Perry *et al.*, Phys. Rev. A **37**, 747 (1988).
- [19] In *Handbook of Chemistry and Physics* (Chemical Rubber, Cleveland, 1965).
- [20] D. N. Fittinghoff *et al.*, Phys. Rev. Lett. **69**, 2642 (1992).
- [21] P. B. Corkum, Phys. Rev. Lett. **71**, 1994 (1993).